The rotational structure of the origin band of the pulsed-field-ionization, zero-kinetic-energy photoelectron spectra of propene-h_6 and propene-d_6

Journal Article

Author(s):
Vasilatou, Konstantina; Schäfer, Mirko; Merkt, Frédéric

Publication date:
2010-10-28

Permanent link:
https://doi.org/10.3929/ethz-a-010782353

Originally published in:
The Journal of Physical Chemistry A 114(42), https://doi.org/10.1021/jp101929d

The following article appeared in *J. Phys. Chem. A* **114**, 11085-11090 (2010) and may be found at http://dx.doi.org/10.1021/jp101929d.

The rotational structure of the origin band of the PFI-ZEKE photoelectron spectra of propene-h_6 and propene-d_6

K. Vasilatou, M. Schäfer, and F. Merkt*

Laboratorium für Physikalische Chemie, ETH Zürich, CH-8092 Zürich, Switzerland

E-mail: merkt@xuv.phys.chem.ethz.ch

Abstract

The pulsed-field-ionization zero-kinetic-energy photoelectron spectra of the origin band of the $\widetilde{\mathrm{X}}^{+\,2}\mathrm{A}'' \leftarrow \widetilde{\mathrm{X}}^{\,1}\mathrm{A}'$ transition of propene (C_3H_6) and perdeuterated propene (C_3D_6) have been recorded at high resolution allowing for the partial resolution of the rotational structure. The analysis of the spectra in the realm of the orbital ionization model for rigid-rotor asymmetric-top molecules enabled the determination of the adiabatic ionization energy of propene and the rotational constants of $C_3H_6^+$ and $C_3D_6^+$. The tunneling splittings resulting from the hindered rotation of the methyl group could not be resolved and the analysis was therefore carried out in the C_s molecular symmetry group. Angular momentum contributions of p_π, d_π and d_δ character were included in the single-center expansion describing the molecular orbital out of which ionization occurs, leading to the selection rules $|\Delta N| = |N^+ - N''| \leq 2$ and $\Delta K_a = K_a^+ - K_a'' = \pm 1, \pm 2$ and to photoelectron partial waves with angular momentum quantum number up to $\ell = 3$. The observation of a strong spectral feature associated with $\Delta K_a = 0$ indicates the importance of vibronic interactions.

*To whom correspondence should be addressed

Introduction

Propene is the simplest molecule having a single methyl rotor adjacent to a carbon-carbon double bond (see Figure 1). It represents a prototypical molecule with which to study hindered rotations and has therefore been studied extensively in the past by various spectroscopic methods. Lide and Mann[1] and Herschbach and Krisher[2] were the first to measure the microwave spectrum of propene and to determine the tunneling splittings associated with the internal rotation of the methyl group. The complete substitution structure of propene (r_s) was derived by Lide and Christensen,[3] who studied seven singly-substituted isotopomers, and was further refined by Hirota and Morino[4] who obtained and analyzed the spectra of several doubly-deuterated species. A full set of rotational constants, centrifugal distortion constants and internal rotation parameters have been determined from microwave and millimeter-wave spectra.[5,6] High-resolution spectroscopic information on several excited vibrational levels of propene has also been reported (see Ref. 7 and references therein). Demaison and Rudolph[7] have calculated the equilibrium structure of propene *ab initio* and compared it to the equilibrium structures derived from experimental results.

Whereas the spectroscopic properties of the electronic ground state of propene are known with high accuracy, no high-resolution spectroscopic information is available on the propene cation. Although the He(I) photoelectron spectrum of propene has been measured and compared to the photoelectron spectra of other monosubstituted ethylenes[8] and several planar unsaturated aliphatic compounds,[9] the vibrational structure of the photoelectron spectrum of the ground state of the propene cation was only resolved recently by Burrill and Johnson[10] using mass-analyzed threshold ionization spectroscopy. Until the present study, no information on the rotational structure of the propene cation was known.

Resolving the rotational structure in the photoelectron spectra of large asymmetric-top molecules represents a considerable experimental challenge, but would be necessary in order to obtain structural information on the cations and, in the case of molecules undergoing large amplitude motions, to study how the removal of an electron affects these motions.

We present here a high-resolution pulsed-field-ionization zero-kinetic-energy (PFI-ZEKE) pho-

toelectron spectroscopic study of the origin band of the $\widetilde{\mathrm{X}}^{+\,2}\mathrm{A}'' \leftarrow \widetilde{\mathrm{X}}^{\,1}\mathrm{A}'$ transition in propene-h_6 and propene-d_6 that enabled us to derive the rotational constants of the cationic species and to determine the adiabatic ionization energy of propene.

Experimental

A vacuum ultraviolet (VUV) laser system[11] with a Fourier-transform-limited bandwidth of better than 0.01 cm^{-1} was used in combination with PFI-ZEKE photoelectron spectroscopy to measure the origin bands of the photoelectron spectra of propene-h_6 and propene-d_6 at high resolution. The laser setup and the procedure for the calibration of the tunable VUV radiation have been described in Refs. 11,12 and only aspects specific to the present study are summarized here. The VUV radiation was generated by resonance-enhanced difference-frequency mixing ($\widetilde{\nu}_{\mathrm{VUV}} = 2\widetilde{\nu}_1 - \widetilde{\nu}_2$) by locking the wave number $\widetilde{\nu}_1$ of the tripled output of a first dye laser to the position $2\widetilde{\nu}_1 =$ 94093.032 cm^{-1} located close to the maximum of the $(4\mathrm{p})^5\,(^2\mathrm{P}_{3/2})\,5\mathrm{p}\,[1/2]\,(J=0) \leftarrow (4\mathrm{p})^6\,(^1\mathrm{S}_0)$ two-photon resonance in krypton. The locking was achieved by stabilizing the fundamental frequency of the dye laser to a neighboring hyperfine component of I_2.[13] The VUV wave number was scanned by tuning the wave number $\widetilde{\nu}_2$ of a second dye laser which was calibrated by recording the laser-induced fluorescence spectrum of I_2. The VUV wave number was determined with an accuracy of better than 0.02 cm^{-1} as the difference $2\widetilde{\nu}_1 - \widetilde{\nu}_2$.

Mixtures of about 20% propene-h_6 (Aldrich, purity $\geq$99%) or propene-d_6 (Aldrich, isotopic purity of 99%) in Ar at a total stagnation pressure of 2.5 bar were introduced into the chamber through a pulsed nozzle (General Valve) and cooled to a rotational temperature of $\approx$ 8 K in a supersonic expansion. The supersonic beam was skimmed and subsequently intersected the VUV laser beam at right angles in the photoionization region.[14]

To achieve high-resolution in the photoelectron spectra, a multipulse electric-field sequence,[15,16] delayed by 2.0 μs relative to the time of photoexcitation and optimized to field ionize narrow slices of the pseudo-continuum of high-n Rydberg states below each ionization threshold, was applied.

The electric fields also accelerated the electrons toward a microchannel-plate detector located at the end of a magnetically shielded time-of-flight tube. In the case of propene-h_6, the pulse sequence consisted of nine electric field steps: a positive discrimination pulse of 167 mV/cm and 1 μs duration, followed immediately by a series of 200-ns-long negative extraction pulses of -100 mV/cm, -142 mV/cm, -167 mV/cm, -183 mV/cm, -208 mV/cm, -233 mV/cm, -500 mV/cm and -1.67 V/cm. A slightly less restrictive pulse sequence with consecutive negative extraction pulses of -117 mV/cm, -150 mV/cm, -183 mV/cm, -217 mV/cm, -250 mV/cm, -283 mV/cm, -500 mV/cm and -1.67 V/cm proved to be more suitable in the case of propene-d_6 because of the weaker photoelectron signal. Eight time gates were set at the positions corresponding to the times of flight of the electrons produced by the negative electric-field pulses and the integrated electron signals were monitored as a function of the laser wave number. The best compromise between high resolution and signal-to-noise ratio was reached in the spectrum obtained with the -167 mV/cm (-183 mV/cm) pulse when measuring propene-h_6 (propene-d_6). A correction of $+1.65$ cm^{-1} ($+1.70$ cm^{-1}) was introduced to compensate for the field-induced shift of the ionization thresholds,[15] which can be determined with an absolute accuracy of ± 0.20 cm^{-1}.

Results and discussion

The PFI-ZEKE photoelectron spectra of the origin band of the $\widetilde{\mathrm{X}}^+ \leftarrow \widetilde{\mathrm{X}}$ transition of propene-h_6 and propene-d_6 are shown in Figure 2 and Figure 3, respectively. Because of the higher degree of spectral congestion and the poorer signal-to-noise ratio of the spectrum of propene-d_6, two PFI-ZEKE photoelectron spectra obtained from two different field ionization pulses (-183 mV/cm and -150 mV/cm) are presented (traces (a) and (c)) to give an impression of the reliability of the measured spectral patterns. The corresponding calculated spectra based on the rovibronic photoionization selection rules presented in Ref. 17 and the orbital ionization model described in Ref. 18 are displayed for comparison below the experimental spectrum in Figure 2 and between

the two experimental spectra in Figure 3.

The rovibronic photoionization symmetry selection rules can be determined from[17]

$$\Gamma''_{\rm rve} \otimes \Gamma^{+}_{\rm rve} \supseteq (\Gamma^{*})^{\ell+1}, \tag{1}$$

where ℓ is the angular momentum of the outgoing photoelectron partial wave, $\Gamma''_{\rm rve}$ ($\Gamma^{+}_{\rm rve}$) represents the irreducible representation of the rovibronic state of the neutral (cation), and Γ^{*} the dipole moment representation of the molecular symmetry group, i.e. the representation which has character -1 for all operations that contain the inversion E^{*} and a character of $+1$ otherwise.[19] Eq. (1) can be expressed in terms of the changes ΔK_a and ΔK_c in the asymmetric-top quantum numbers K_a and K_c. The principal axis system chosen to classify the rotational levels of propene is depicted in Figure 1 (see also Ref. 3) and corresponds to the convention I$^{\rm r}$.[20] This choice results in the following selection rules for the $\widetilde{\rm X}^{+}(0^0, \Gamma^{+}_{\rm ve} = {\rm A}'') \leftarrow \widetilde{\rm X}(0^0, \Gamma''_{\rm ve} = {\rm A}')$ ionizing transition of propene in the $C_{\rm s}$ molecular symmetry group:

$\Delta K_a = K_a^{+} - K_a^{''} =$ even/odd, $\Delta K_c = K_c^{+} - K_c^{''} =$ odd for $\ell =$ odd

$\Delta K_a = K_a^{+} - K_a^{''} =$ even/odd, $\Delta K_c = K_c^{+} - K_c^{''} =$ even for $\ell =$ even.

The rovibronic symmetry selection rules depend on the parity of the outgoing electron partial wave because even-ℓ partial waves transform as A$'$ and odd-ℓ partial waves as A$''$ ($= \Gamma^{*}$ in the $C_{\rm s}$(M)).

The experimental resolution of about 0.15 cm^{-1} achieved in the present measurements allowed for the partial resolution of the rotational structure of the photoelectron spectra (see Figure 2 and Figure 3). To analyze the structure observed in the spectrum of C_3H_6, the rotational constants of the neutral ground state derived in Ref. 5 from a global fit of A and E lines observed in the microwave and millimeter wave spectra were adopted. The adiabatic ionization energy and the rotational constants of the cationic ground state were then optimized in an iterative procedure in which the temperature and the relative intensities of the different branches were also modified.

Once a satisfactory agreement between observed and calculated spectra was reached, ten lines of the experimental spectrum corresponding to single transitions were identified and used to refine

the rotational constants of the ion and the adiabatic ionization energy in a least-squares fit (see Table 1). The fit yielded the results summarized in the fourth row of Table 2. A final slight adjustment of the rotational constants was then undertaken which yielded the calculated spectrum presented in Figure 2 (trace (b)) and the set of spectroscopic constants listed in the third row of Table 2. The uncertainties in these parameters represent the range of parameter values for which the agreement between the calculated and measured spectra is satisfactory.

The value of the adiabatic ionization energy of propene-h_6 determined here (78602.00(40) cm^{-1}) differs by approximately 15 cm^{-1} from the value reported in Ref. 10. We have no explanation for this discrepancy.

The assignment bar given above the experimental trace displayed in Figure 2 designates only contributions arising from $\Delta N = N^+ - N'' = 0$, namely 'Q-type' branches, while the associated change in K_a is given below the assignment bar in the notation $K_a'' \rightarrow K_a^+$. In the case of a near prolate top, the pattern-forming quantum number is K_a. The calculated spectrum (trace (b)) was therefore decomposed into groups of transitions that share the same values of K_a'' and K_a^+ (traces (d)–(h)). Traces (d)–(h) are related to a change in K_a of ± 1 and exhibit characteristic branches for all possible values of ΔN. As an illustration, the individual transitions have been grouped in trace (e) according to the value of ΔN which represents the change in total angular momentum excluding spins and further labeled below the assignment bar according to the quantum number N''.

The orbital ionization model described in Ref. 18 (specifically Eq. (7), of Ref. 18) was used to calculate the rotational intensity distributions of the spectra. In this model, the angular momentum of the photon is assumed to be fully absorbed by the outgoing photoelectron, creating a hole of the same angular-momentum composition as the molecular orbital out of which ionization occurs. In the present case, this molecular orbital has a nodal plane containing the three C atoms and is of a'' symmetry in the C_s molecular symmetry group. Moreover, the C-C double bond is not aligned with the principal axis ($z = a$-axis) and the center of mass is displaced with respect to the central carbon atom (see Figure 1). This implies that the single-center expansion describing this molecular orbital can have contributions from all atomic-like orbitals that conserve the nodal plane, i.e., orbitals that

have a quantum number $|\lambda^{''}| > 0$ for the projection of the angular momentum of the molecular orbital onto the principal axis, denoted with the subscripts π (for $\lambda^{''} = \pm 1$), δ (for $\lambda^{''} = \pm 2$), etc. The single-center expansion was truncated to include only the most significant contributions of $\ell'' = 1$, $\lambda'' = \pm 1$ (p_π), $\ell'' = 2$, $\lambda'' = \pm 1$ (d_π), and $\ell'' = 2$, $\lambda'' = \pm 2$ (d_δ) angular momentum character, leading to the selection rules $|\Delta N| = |N^+ - N^{''}| \leq 2$ and $\Delta K_a = K_a^+ - K_a^{''} = \pm 1, \pm 2$.

However, to reproduce the intensity of the central prominent peak of the experimental spectrum an additional contribution corresponding to a fictive $\ell'' = 0$, $\lambda'' = 0$ component had to be included in the simulations, leading to the $\Delta K_a = \Delta N = 0$ contribution depicted as a dashed line in Figure 2 and a dotted line in Figure 3. The necessity to include this contribution despite the fact that the highest occupied molecular orbital does not possess any s character for symmetry reason indicates the importance of vibronic mixing and/or configuration interactions. That configuration interactions or vibronic mixing occur is also implied by the observation of vibrational bands of A$''$ symmetry in the photoelectron spectrum of the $\widetilde{X}^+\,^2A''$ state of $C_3H_6^+$ (see Ref. 10). The best agreement with the experimental spectrum of propene-h_6 could be achieved for a rotational temperature of ≈ 8 K and by taking into account the following four angular momentum components: $(\ell'', \lambda'') = (0,0), (1, \pm 1), (2, \pm 1)$ and $(2, \pm 2)$ with weights of 0.4, 0.3, 1.3 and 0.6, respectively.

The same weights with a rotational temperature of ≈ 7 K were also used to calculate the intensity distributions observed in the PFI-ZEKE photoelectron spectrum of the origin band of the $\widetilde{X}^+ \leftarrow \widetilde{X}$ transition in C_3D_6 displayed in Figure 3 (traces (a) and (c)). The rotational structure and assignment are similar to those of propene-h_6 with the main difference that the spectral congestion is more pronounced. Perdeuterated propene has not been studied by microwave spectroscopy and consequently the rotational constants of the neutral ground state had to be estimated in order to reproduce the rotational structure of the cation in our calculations. Using the substitution structure derived in Ref. 3, the differences in the moments of inertia $\Delta I_i (i = a, b, c)$ between propene-h_6 and its fully deuterated isotopomer could be calculated.[21] The moments of inertia of C_3D_6 were then

determined according to the relation:

$$I_i(d_6)(\text{calc.}) = \Delta I_i + I_i(h_6)(\text{expt.}), \tag{2}$$

where $I_i(h_6)$(expt.) are the moments of inertia of C_3H_6 determined in Ref. 5. The calculated rotational constants of neutral perdeuterated propene are listed in the lower part of Table 2. The accuracy of these rotational constants is amply sufficient for the present purpose and their values were therefore kept fixed in the analysis of the experimental spectrum. Following the same procedure as described above for C_3D_6 led to the values of the adiabatic ionization energy and the rotational constants of the cationic ground state summarized in the last row of Table 2.

The calculated spectra presented in Figure 2 and Figure 3 capture the main features of the experimental spectra and reproduce the relative intensities of the transitions satisfactorily. At the rotational temperature of $7-8$ K assumed in the simulations, only ground-state levels with $N'' \leq 10$ and $K_a'' \leq 4$ contribute significantly to the spectrum. At our experimental resolution and at this low rotational temperature, the centrifugal distortion terms can be neglected in the rotational Hamiltonian. The comparison of experimental and calculated spectra of the origin band of the $\widetilde{X}^+$ state of $C_3H_6^+$ (Figure 2) reveals that several spectral features are broader in the former spectrum than in the latter. Tunneling splittings arising from the internal rotation of the methyl group, unresolved spin-rotation splittings and intensity perturbations by channel interactions[22] are possible reasons for the broadening of these peaks. The good overall agreement between experimental and calculated spectra shows that their effect is small and that the (unresolved) splittings must be less than 0.15 cm^{-1}.

Conclusions

The present study of the origin band of the $\widetilde{X}^+ \leftarrow \widetilde{X}$ transition of the photoelectron spectrum of propene and its fully deuterated isotopomer has enabled the determination of the first adiabatic ionization energy and the derivation of the rotational constants of both $C_3H_6^+$ and $C_3D_6^+$. The analysis

of the rotational structure in the photoelectron spectra was based on a rigid-rotor model because the effects arising from the internal rotation of the methyl group and centrifugal distortions could not be observed at our experimental resolution and at the low temperature of the sample. The molecular orbital out of which ionization occurs was described as a linear combination of p_π, d_π, and d_δ atomic-like orbitals with origin at the center of mass of the molecule. To successfully reproduce the experimental intensity distributions, a contribution of s angular momentum character had to be included in the single-center expansion of the highest occupied (a'') molecular orbital. The inclusion of this angular momentum component, which is nominally forbidden in C_s symmetry, suggests that vibronic interactions are important in the description of the photoionization dynamics of propene and may even indicate a possible distortion from a C_s structure. Further experimental and *ab initio* investigations would be required to provide insight into these interactions.

The development of ZEKE photoelectron spectroscopy by Müller-Dethlefs *et al.*[23] 25 years ago was an important step in the evolution of photoelectron spectroscopy toward a spectroscopic method with which information on the rovibrational energy level structure of molecular cations can be obtained. Thanks to the continual improvement of its resolution resulting from the exploitation of electric field ionization sequences,[15,24,25] PFI-ZEKE photoelectron spectroscopy, initially applied to resolve the rotational structure in the photoelectron spectra of diatomic molecules, has rapidly been applied to obtain information on the rovibrational photoionization of more complex molecules: first symmetric-top molecules such as ammonia,[26] benzene[25,27] and benzene-rare-gas van der Waals molecules[28] and then small asymmetric-top molecules such as H_2O,[29] O_3,[30] ethene,[31,32] and allene.[33]

The present results on propene illustrate the possibility of partially resolving the rotational structure in single-photon photoelectron spectra of structurally more complex molecules. This possibility results in the following advantages: The rotational structure of a photoelectron spectrum enables the determination of the vibronic symmetry of the cationic states by means of rovibronic photoionization selection rules; it permits the distinction between different conformers of the neutral or ionized molecule, it gives access to the rovibronic photoionization dynamics and provides

information on the electronic structure.

Acknowledgement

The authors thank Dr. J. M. Michaud and Dr. U. Hollenstein (both ETH Zurich) for experimental help. This work is supported financially by the Swiss National Science Foundation under project Nr. 200020-125030 and the ETH Zurich.

Captions

Figure 1: Propene and its principal inertial axes in the I^r convention for near-prolate asymmetric tops.

Figure 2: Trace (a): PFI-ZEKE photoelectron spectrum of the origin band of the $\widetilde{X}^+\,^2A'' \leftarrow \widetilde{X}\,^1A'$ transition of C_3H_6. Trace (b): Calculated spectrum using a Gaussian instrument function of full width at half maximum of 0.15 cm^{-1}. Trace (c): Estimated $\Delta K_a = 0$ contribution to the spectrum. Traces (d)–(h): Calculated contributions to the overall intensity distribution associated with specific values of K_a'' and K_a^+ as indicated above each trace.

Figure 3: Trace (a): PFI-ZEKE photoelectron spectrum of the origin band of the $\widetilde{X}^+\,^2A'' \leftarrow \widetilde{X}\,^1A'$ transition of C_3D_6 obtained by monitoring the electrons released by the -183 mV/cm field-ionization step of the pulse sequence. The assignment bar designates only branches associated with a change in the total angular momentum $\Delta N = 0$. The change in K_a is given below the assignment bar in the notation $K_a'' \rightarrow K_a^+$. Trace (b): Calculated spectrum using a Gaussian instrument function with a FWHM of 0.2 cm^{-1}. The dotted line represents the estimated $\Delta K_a = 0$ contribution. Trace (c): Spectrum obtained by monitoring the electrons released by the -150 mV/cm step of the pulse sequence. The spectrum was recorded simultaneously with trace (a). Trace (c) was shifted by -0.15 cm^{-1} along the horizontal axis to compensate for the difference in the field-induced shifts of the ionization thresholds (see text for more details).

Table 1: Observed ($\widetilde{\nu}_{expt.}$) and calculated ($\widetilde{\nu}_{calc.}$) line positions of the well-resolved lines in the PFI-ZEKE photoelectron spectrum of the origin band of the $\widetilde{X}^+\,^2A'' \leftarrow \widetilde{X}\,^1A'$ transition of C_3H_6.

$\widetilde{\nu}_{\rm fit}$ represents the positions determined from the least-squares fit based on the ten well-resolved lines only. The positions have not been corrected for the -1.65 cm^{-1} field-induced shift of the ionization thresholds (see text for details).

Table 2: Adiabatic ionization energies and rotational constants obtained from the analysis of the rotational structure of the origin band of the $\widetilde{\rm X}^{+\,2}{\rm A}'' \leftarrow \widetilde{\rm X}\,^1{\rm A}'$ ionizing transition of C_3H_6 and C_3D_6.

References

(1) Lide, Jr., D. R.; Mann, D. E. *J. Chem. Phys.* **1957**, *27*, 868–873.

(2) Herschbach, D. R.; Krisher, L. C. *J. Chem. Phys.* **1958**, *28*, 728–729.

(3) Lide, Jr., D. R.; Christensen, D. *J. Chem. Phys.* **1961**, *35*, 1374–1378.

(4) Hirota, E.; Morino, Y. *J. Chem. Phys.* **1966**, *45*, 2326–2327.

(5) Wlodarczak, G.; Demaison, J.; Heineking, N.; Császár, A. G. *J. Mol. Spectrosc.* **1994**, *167*, 239–247.

(6) Pearson, J. C.; Sastry, K. V. L. N.; Herbst, E.; De Lucia, F. C. *J. Mol. Spectrosc.* **1994**, *166*, 120–129.

(7) Demaison, J.; Rudolph, H. D. *J. Mol. Spectrosc.* **2008**, *248*, 66–76.

(8) Mollère, P.; Bock, H.; Becker, G.; Fritz, G. *J. Organometal. Chem.* **1972**, *46*, 89–96.

(9) Kimura, K.; Katsumata, S.; Yamazaki, T.; Wakabayashi, H. *J. Electron Spectrosc. Relat. Phenom.* **1975**, *6*, 41–52.

(10) Burrill, A. B.; Johnson, P. M. *J. Chem. Phys.* **2001**, *115*, 133–138.

(11) Hollenstein, U.; Palm, H.; Merkt, F. *Rev. Sci. Instr.* **2000**, *71*, 4023–4028.

(12) Hollenstein, U.; Seiler, R.; Merkt, F. *J. Phys. B: At. Mol. Opt. Phys.* **2003**, *36*, 893–903.

(13) Paul, Th. A.; Liu, J.; Merkt, F. *Phys. Rev. A* **2009**, *79*, 022505.

(14) Signorell, R.; Palm, H.; Merkt, F. *J. Chem. Phys.* **1997**, *106*, 6523–6533.

(15) Hollenstein, U.; Seiler, R.; Schmutz, H.; Andrist, M.; Merkt, F. *J. Chem. Phys.* **2001**, *115*, 5461–5469.

(16) Hollenstein, U.; Seiler, R.; Osterwalder, A.; Sommavilla, M.; Wüest, A.; Rupper, P.; Willitsch, S.; Greetham, G. M.; Brupbacher-Gatehouse, B.; Merkt, F. *Chimia* **2001**, *55*, 759–762.

(17) Signorell, R.; Merkt, F. *Mol. Phys.* **1997**, *92*, 793–804.

(18) Willitsch, S.; Merkt, F. *Int. J. Mass Spectrom.* **2005**, *245*, 14–25.

(19) Bunker, P. R.; Jensen, P. *Molecular Symmetry and Spectroscopy*, 2nd ed.; NRC Research Press: Ottawa, 1998.

(20) Zare, R. N. *Angular Momentum*; John Wiley & Sons: New York, 1988.

(21) Nösberger, P.; Bauder, A.; Günthard, Hs. H. *Chem. Phys.* **1973**, *1*, 418–425.

(22) Merkt, F.; Softley, T. P. *Int. Rev. Phys. Chem.* **1993**, *12*, 205–239.

(23) Müller-Dethlefs, K.; Sander, M.; Schlag, E. W. *Chem. Phys. Lett.* **1984**, *112*, 291–294.

(24) Chupka, W. A. *J. Chem. Phys.* **1993**, *98*, 4520–4530.

(25) Dietrich, H.-J.; Müller-Dethlefs, K.; Baranov, L. Y. *Phys. Rev. Lett.* **1996**, *76*, 3530–3533.

(26) Reiser, G.; Habenicht, W.; Müller-Dethlefs, K. *J. Chem. Phys.* **1993**, *98*, 8462–8468.

(27) Ford, M.; Lindner, R.; Müller-Dethlefs, K. *Mol. Phys.* **2003**, *101*, 705–716.

(28) Siglow, K.; Neuhauser, R.; Neusser, H. J. *J. Chem. Phys.* **1999**, *110*, 5589–5599.

(29) Wang, K.; Lee, M.-T.; McKoy, V.; Wiedmann, R. T.; White, M. G. *Chem. Phys. Lett.* **1994**, *219*, 397–404.

(30) Willitsch, S.; Innocenti, F.; Dyke, J. M.; Merkt, F. *J. Chem. Phys.* **2005**, *122*, 024311.

(31) Willitsch, S.; Hollenstein, U.; Merkt, F. *J. Chem. Phys.* **2004**, *120*, 1761–1774.

(32) Wang, P.; Xing, X.; Baek, S. J.; Ng, C. Y. *J. Phys. Chem. A* **2004**, *108*, 10035–10038.

(33) Schulenburg, A. M.; Merkt, F. *J. Chem. Phys.* **2009**, *130*, 034308.

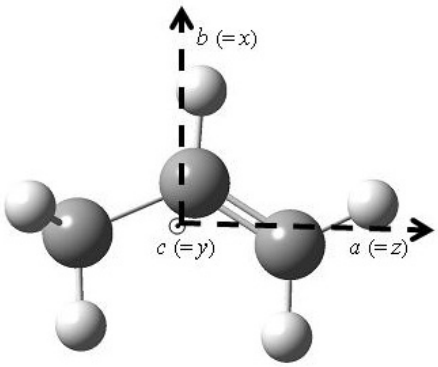

Figure 1

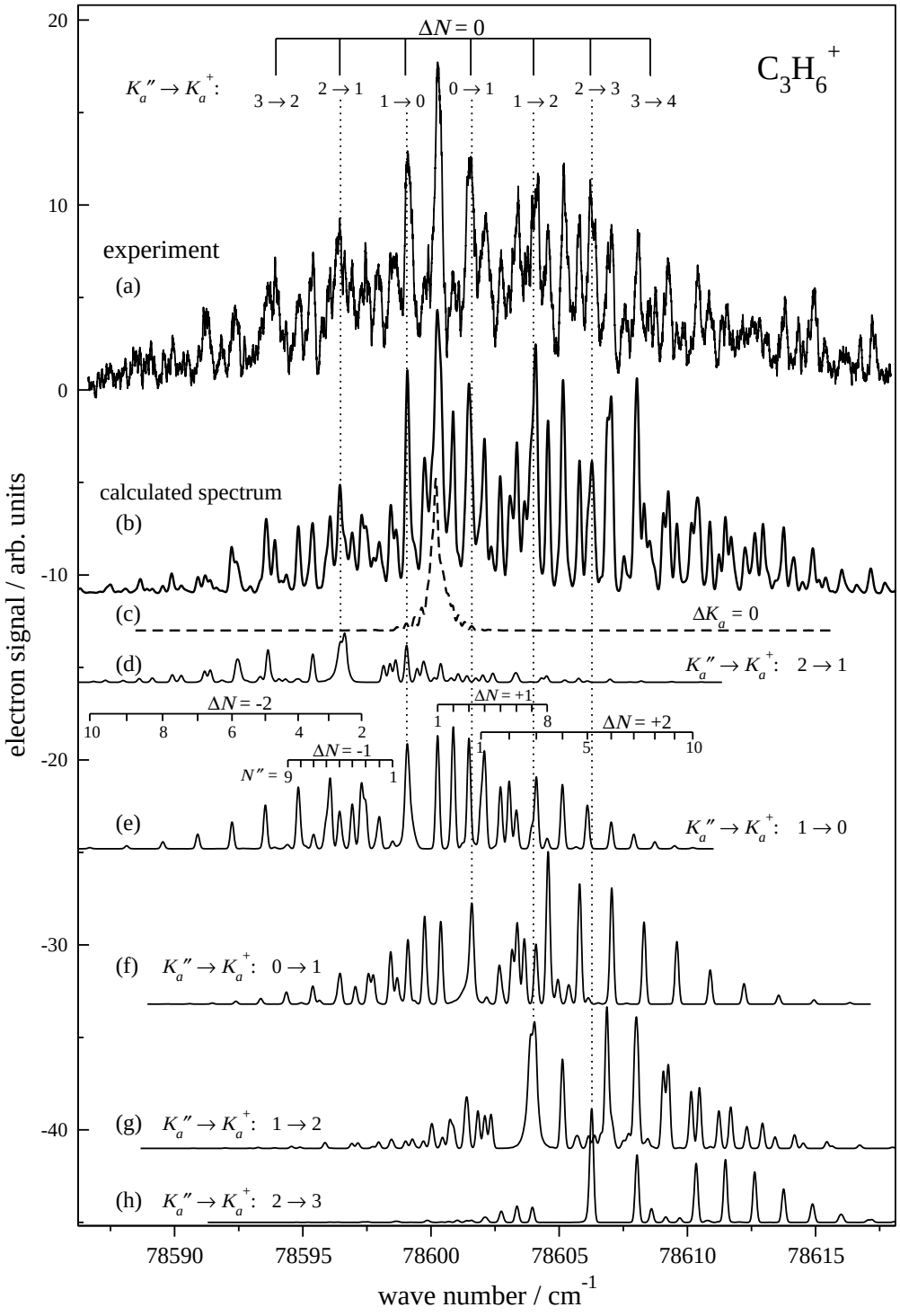
ΔN = 0
$K_a'' \rightarrow K_a^+$:
3 → 2
2 → 1
1 → 0
0 → 1
1 → 2
2 → 3
3 → 4
$C_3H_6^+$
experiment
(a)
calculated spectrum
(b)
(c)
ΔK_a = 0
(d)
$K_a'' \rightarrow K_a^+$: 2 → 1
ΔN = -2
ΔN = +1
ΔN = +2
ΔN = -1
N'' = 9
(e)
$K_a'' \rightarrow K_a^+$: 1 → 0
(f) $K_a'' \rightarrow K_a^+$: 0 → 1
(g) $K_a'' \rightarrow K_a^+$: 1 → 2
(h) $K_a'' \rightarrow K_a^+$: 2 → 3
electron signal / arb. units
wave number / cm^{-1}

Figure 2

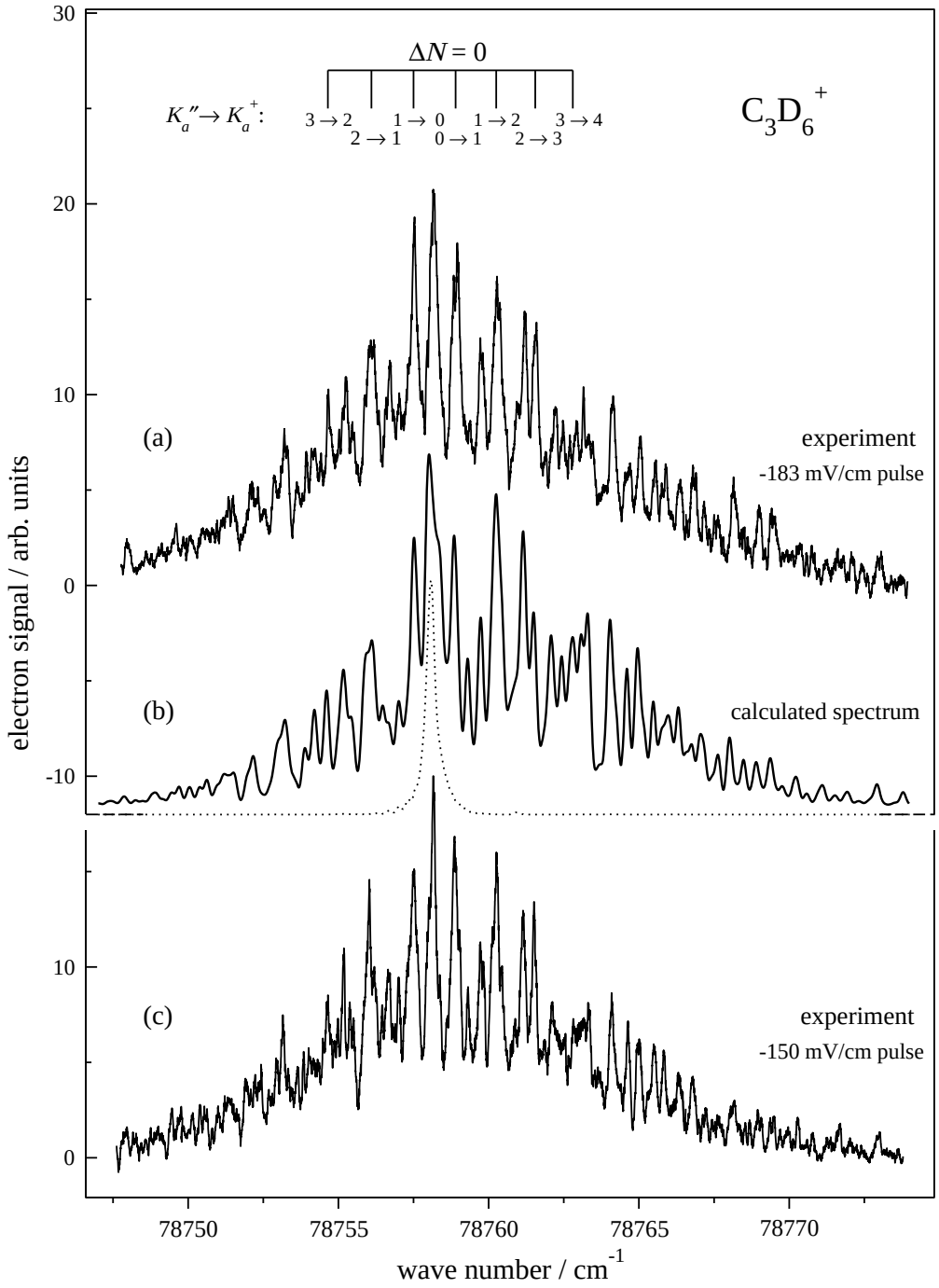
ΔN = 0
$K_a'' \rightarrow K_a^+$:
3 → 2
2 → 1
1 → 0
0 → 1
1 → 2
2 → 3
3 → 4
$C_3D_6^+$
(a)
experiment
-183 mV/cm pulse
(b)
calculated spectrum
(c)
experiment
-150 mV/cm pulse
electron signal / arb. units
wave number / cm^{-1}
30
20
10
0
-10
10
0
78750
78755
78760
78765
78770

Figure 3

Table 1

$N''_{K''_a K''_c}$	$N^+_{K^+_a K^+_c}$	$\widetilde{\nu}_{\text{expt.}}$	$\widetilde{\nu}_{\text{calc.}} - \widetilde{\nu}_{\text{expt.}}$	$\widetilde{\nu}_{\text{fit}} - \widetilde{\nu}_{\text{expt.}}$
7_{16}	5_{05}	78590.95	-0.05	0.00
4_{13}	2_{02}	78594.85	-0.03	-0.06
3_{12}	1_{01}	78596.00	0.07	0.03
2_{02}	4_{13}	78605.80	0.00	-0.02
3_{03}	5_{14}	78607.01	0.04	0.03
3_{12}	5_{23}	78609.09	-0.03	0.00
3_{13}	5_{24}	78609.25	0.01	0.05
5_{14}	7_{25}	78611.35	-0.12	-0.03
3_{21}	5_{32}	78611.55	-0.07	-0.02
3_{22}	5_{33}	78611.55	-0.06	-0.01

Table 2

	E_i/cm^{-1}	A/cm^{-1}	B/cm^{-1}	C/cm^{-1}	
C_3H_6 neutral		1.54377219(18)	0.310492638(37)	0.271196772(40)	Ref. 5
$C_3H_6^+$ 0^0	78602.00(40)	1.508(10)	0.309(6)	0.267(6)	This work [a]
	78601.96	1.513	0.309	0.273	This work[b]
	78587(4)				Ref. 10
C_3D_6 neutral		0.9202	0.2395	0.2042	This work[c]
$C_3D_6^+$ 0^0	78759.90(50)	0.903(7)	0.236(5)	0.201(5)	This work[d]

[a]Values obtained from the analysis of the rotational structure of the origin band of the $\widetilde{X}^+\,^2A'' \leftarrow \widetilde{X}\,^1A'$ transition of C_3H_6. The value of the adiabatic ionization energy of C_3H_6 has been corrected for the field-induced shift. The numbers in parentheses represent the estimated uncertainties.
[b]Values obtained from a least-squares fit of the spectroscopic constants to the positions of the ten well-resolved lines of the PFI-ZEKE photoelectron spectrum of the origin band of the $\widetilde{X}^+\,^2A'' \leftarrow \widetilde{X}\,^1A'$ transition of C_3H_6.
[c]Parameters were kept fixed to the calculated values.
[d]Values obtained from the analysis of the rotational structure of the origin band of the $\widetilde{X}^+\,^2A'' \leftarrow \widetilde{X}\,^1A'$ transition of C_3D_6. The value of the adiabatic ionization energy of C_3D_6 has been corrected for the field-induced shift. The rotational constants are correlated with those of the neutral molecule and therefore the values obtained and their uncertainties result from the values chosen for the neutral ground state.